Title

XPS OP NON-HEME IRON PROTEINS. INVESTIGATION OF THE IRON-SULFUR MOEITY IN NON-HEME IRON PROTEINS BY MEANS OF X-RAY PHOTOELECTRON SPECTROSCOPY

Authors

Kramer, Leo N.
Klein, Melvin P.

Publication Date

1971-08-01

Submitted to Journal of
Biological Chemistry

LBL-302
Preprint

XPS OF NON-HEME IRON PROTEINS. INVESTIGATION OF THE IRON-SULFUR MOEITY IN NON-HEME IRON PROTEINS BY MEANS OF X-RAY PHOTOELECTRON SPECTROSCOPY

Leo N. Kramer and Melvin P. Klein

August 1971

AEC Contract No. W-7405-eng-48

LBL-302

LAWRENCE RADIATION LABORATORY
UNIVERSITY of CALIFORNIA BERKELEY

DISCLAIMER

XPS of Non-heme Iron Proteins

Investigation of the iron-sulfur moiety in non-heme iron proteins by means of X-ray photoelectron spectroscopy.

Leo N. Kramer and Melvin P. Klein

Laboratory of Chemical Biodynamics, Lawrence Berkeley Laboratory,

University of California, Berkeley, California 94720*

*This work was supported, in part, by the U. S. Atomic Energy Commission.

SUMMARY

In this paper are presented the X-ray photoelectron (XPS) spectra of four non-heme iron proteins: rubredoxin, HIPIP, clostridial ferredoxin, and spinach ferredoxin. XPS spectra from model complexes, and extended Hückel calculations of hypothetical and synthesized complexes have been used to interpret these protein spectra with respect to the structure-function relationship of the proteins' active moieties. XPS spectra of rubredoxin exhibited relatively high binding energies (B.E.s) for the iron and sulfur atoms and only one sulfur peak, which is compatible with a structure consisting of one iron atom surrounded by four sulfur atoms. The XPS spectra of the other three proteins investigated exhibited relatively low B.E.s for the iron atoms and two sulfur peaks, which is compatible with a structure consisting of a clustered arrangement of iron and sulfur atoms.

The non-heme iron proteins, collectively referred to as the ferredoxins, have received considerable attention in recent years because of their unusual properties. The biochemical interest derives from their extreme values of redox potential which nature has exploited by their incorporation into several electron transport chains. The biochemical investigations have been summarized in recent reviews (1,2). Several types of physical measurements have been performed, the objectives of which have been to elucidate those features of the molecular, atomic and electronic structure responsible for the biochemical properties. Table I lists some pertinent physical properties of these proteins. The chemical and physical investigations on these proteins have been reviewed by Tsibris and Woody (3). The work reported here, employing a relatively new class of physical measurement, was engendered in the same spirit of probing further into the structure-function relationship of these intriguing molecules.

When this work was initiated it was known that the proteins contained non-heme iron, acid labile sulfur and cysteine sulfur. The absorption spectra of the intact proteins exhibited features which changed in a characteristic and reversible manner upon reduction (or oxidation). Since these features were totally absent in the apo-proteins, it was concluded that the iron and probably certain of the sulfurs were at the active site. Subsequently, the elegant EPR experiments deriving from Beinert and collaborators (4,5) which employed isotopes of iron and sulfur, and replacement of the labile sulfur with selenium, showed conclusively that these elements were indeed at the EPR site and presumably at the active site. There has thus evolved a picture that the active site(s) contain an iron-sulfur complex or clusters.

The problem which we addressed was to examine the iron and sulfur moieties by X-ray photoelectron spectroscopy (XPS). This method permits a study of each element specifically and individually, and is capable of providing some structural and bonding information rather more directly than is accessible from any other contemporary form of spectroscopy. We have applied this method to four non-heme iron proteins: rubredoxin, "high potential iron protein" (HIPIP), clostridial ferredoxin, and spinach ferredoxin. These four were chosen as representative of all the currently known iron-sulfur proteins. XPS data from model complexes which correlate well with theory are used to aid in the interpretation of the protein spectra.

The first section of the paper describes the physical method. The second discusses the experimental procedures. We then present the experimental results, followed by a discussion and interpretation, and conclude with a summary of the findings.

METHODS

When a sample is irradiated with light of sufficient energy, electrons may be ejected and their kinetic energy is given by the well known Einstein relation,

$$K.E. = h\nu - B.E.,$$

where K.E. is the kinetic energy of the electrons, h is Planck's constant, ν is the frequency of the light quantum, and B.E. is the binding energy of the electrons in the sample. If the photon energy is increased sufficiently, by using X-rays, electrons may be ejected from the inner or core levels of the constituent atoms of the sample. Since photon or X-ray

energies are known to high accuracy, the binding energies may be determined with precision by measurement of the kinetic energies. The measurements may be performed with a variety of devices, but most commonly magnetic and electrostatic deflection analyzers are employed. The overwhelming majority of the energy levels of the elements across the periodic table have been determined in this manner.

The method is outlined schematically in Figure 1. In this figure are sketched the discrete energy levels of a particular atom in a compound as well as those levels which are a collective property of the compound as a whole and make up its valence band or molecular orbitals. An X-ray photon is shown lifting an electron from the 2S level of this atom into the continuum of energies, or, equivalently, removing it to infinity. At this point the electron enters the spectrometer, wherein it is brought to a focus and impinges on a detector when the electron has the correct energy (more rigorously the correct momentum). The energy range is scanned by varying the strength of the magnetic field and thus a spectrum is traced out by recording the number of electrons reaching the detector at each value of the magnetic field in complete analogy with mass spectrometry. This method was developed and brought to its present state of refinement by the group at the Institute of Physics at the University of Uppsala, Sweden (6).

Since all atoms are constructed in the same manner, it is possible to photoeject their electrons, and by a suitable choice of exciting X-ray energy and particular atomic level one can distinguish among the different constituent atoms of the sample. It is apparent, then, that calibration against a sample of known elementary composition will permit

a qualitative and quantitative analysis of the unknown sample. The absolute sensitivity of the method is very high, although it is not especially suitable for detecting small amounts of one element in the presence of a large excess of other elements.

More recently it has been shown that a given element in different chemical configurations exhibits chemical shifts of its binding energies (7). These chemical shifts thus extend significantly the utility of the method so that not only the total quantity of a given element may be determined, but also the type or types of chemical bonding situation in which the atom is located. The origins and theoretical foundations for these chemical shifts are rather well understood (7,8). An intuitive understanding of the chemical shifts may be derived from the following simple argument. In a neutral atom the electron binding energies are determined by the attractive potential between the electrons and the positive nucleus and the repulsive interactions among the electrons. In a normal complex the valence electrons are partially donated to or accepted from the ligating atoms. The net effect in a particular complex is a decrease or increase of the net charge on the atom under study relative to the charge on this atom in other complexes. This change of net charge is accompanied by an increase or decrease of the binding energies of the core electrons. More formal and detailed arguments will be found in the literature references and will be presented in the discussion section.

EXPERIMENTAL PROCEDURE

Spinach ferredoxin was prepared by the method of Tagawa and

Arnon (9). Clostridial ferredoxin and clostridial apoferredoxin were obtained from Prof. J. C. Rabinowitz, HIPIP from Dr. R. G. Bartsch, and rubredoxin from Dr. W. Lovenberg.

All spectra were produced and analyzed in the Berkeley iron-free photoelectron spectrometer (10). In order to obtain spectra from proteins in a state approximating the solution and to obviate the interfering effects of $SO_4^=$ accompanying $(NH_4)_2SO_4$ precipitation, the samples were run in frozen buffered aqueous solution. An accessory transfer chamber, which allowed controlled cooling of the samples, was used in the spectrometer source housing (11). The solutions were frozen to about -90°C before submitting them to the spectrometer vacuum of about 10^{-5} torr. Each ferredoxin spectrum represents the best data obtained from experiments with from three to five different samples of the same protein. Spectra composed of several peaks were resolved by curve-fitting with lorentzian lines of restricted half-widths by means of a computer program described elsewhere (12).

X-ray doses of 10^5 r. are known to decompose cystine and cysteine in aqueous solution at room temperature (13). Radiation decomposition of amino acids in the dry, solid state in air is also known to occur (13). Experiments were carried out to determine the radiation dose to which the samples in our spectrometer were subjected. Exposure of a radiation safety film badge to the conditions of a typical experiment indicated a maximum dose rate of approximately 10^3 rads/hr. To determine the effect of this quantity of radiation on the proteins, samples of spinach ferredoxin, frozen to dry ice temperatures, were subjected to a dose of 3×10^4 rads of Co^{60} γ-rays. These experiments showed that the biological activity of the irradiated sample, as determined by the rate of NADP

reduction (9), decreased approximately 10 to 15% from an unirradiated control sample. As all of the spectra presented in this paper were obtained within 12 hours, bulk decomposition does not appear to be a serious factor.

The purity of the ferredoxin samples, from which XPS spectra were obtained, was checked optically. All samples had purity ratios within 10% of the optimum literature values. The optical purity ratios of the samples, before and after XPS spectra were obtained, appeared to remain constant to within 10%. However, XPS spectra result from the top few hundred angstroms of the sample surface (7), and degradation in only these layers would be difficult to detect by an optical method (since only a fraction of the sample would be affected). These top layers are submitted not only to an X-ray flux of about 1000 rads/hr, but are also susceptible to freeze-drying effects and possibly surface reactions (although measures were taken to avoid the freeze-drying phenomenon) (11). The spectra presented here were consistently reproducible using about three different samples for each protein, and the corresponding spectra did not deteriorate significantly with time. Thus, the proteins investigated by this XPS method did not explicitly show the effects of decomposition.

EXPERIMENTAL RESULTS

Figure 2 shows the S2P photoelectron spectra of the four non-heme iron proteins under investigation and also that of clostridial apoferredoxin. This apoferredoxin was prepared in the laboratory of Dr. J. C. Rabinowitz by removing the iron and labile sulfur from clostridial ferredoxin, leaving only cystine groups in the protein (14).

The corresponding Fe3P photoelectron spectra are shown in Figure 3. These spectra have been adjusted by subtracting out a constant background from the raw data. It should be noted that the typical Fe3P spectrum displays a half-width of about 2.8 eV. However, the apparent broadening in the iron spectra of these proteins is not necessarily due to the existence of chemically or magnetically different iron species, but may result from the very poor statistical resolution of the Fe3P photoelectrons from these proteins.

Table II summarizes the quantitative results of these iron and sulfur spectra. The estimated error to the measured B.E.s is the scatter of values obtained from several experiments with each protein. The area ratios have also been estimated by considering all experimental spectra but, nevertheless, are only a rough estimate and are not to be taken as precisely accurate.

These non-heme iron proteins were reduced using $Na_2S_2O_3$ (or, in the case of HIPIP, oxidized with $K_3Fe(CN)_6$) and investigated as frozen solutions. However, no significant change in the photoelectron spectra could be detected upon reducing or oxidizing the proteins. However, in many cases the reduced proteins showed significant decomposition after exposure to the experimental conditions and thus unequivocal interpretation of the effects of reduction upon the XPS spectra was not possible.

Possible model ligating systems of the iron-sulfur complex in the non-heme iron proteins are presented in Tables III and IV. Table III contains the measured Fe3P and S2P B.E.s and calculated charges of synthesized model iron-sulfur complexes. Table IV contains the calculated iron and sulfur charges of hypothetical model iron-sulfur complexes. The data of Tables II, III, and IV are summarized by Figure 4, in which the B.E.s of

the non-heme iron proteins are represented as short lines within the semicircles. The uncertainty in these B.E.s is represented by the length of these lines. Model complexes from Table IV are abbreviated by the notation M.C. in Figure 4.

To provide background information for use in the interpretation of the protein spectra, the iron and sulfur photoelectron spectra of a diverse series of compounds of known stoichiometry and structure were collected. In a previous publication we have presented these results together with an interpretation based upon the extended Hückel theory (15). These data are presented in Table V and Figure 5. We will consider these model data in the Discussion section.

DISCUSSION

The photoelectron spectrum of a chemical system should give insight into the electronic structure of that system, since changes in chemical environment of an atom will correspondingly change the B.E.s of its core electrons (7). When interpreting our XPS data we use the assumption that similar atomic binding energies represent similar chemical environments. Although this assumption is necessary, it is not sufficient alone for interpreting XPS spectra. Molecular orbital calculations of atomic binding energies or parameters related to B.E.s in synthesized and hypothetical model complexes can also be helpful in substantiating the interpretation of the XPS spectra. We have established, in a separate publication (15), direct correlations between electron B.E. and atomic charge, calculated by means of extended Hückel theory, for a diverse series of iron and sulfur compounds.

Atomic charges and binding energies of the model complexes were calculated using the extended Hückel method formulated by Hoffmann (16,17), with modifications to the Coulomb integrals and Slater exponents such that iteration to charge self-consistency could be obtained. This method does not include electron repulsion terms explicitly, and uses empirical parameters for evaluating the elements of the secular determinant. Table V shows a direct correlation between calculated B.E. and calculated charge. From this observation it seems reasonable to expect similar results for attempts to correlate measured electron B.E.s with either calculated charge or calculated electron B.E.s. However, the correlations are admittedly somewhat artificial since the simple extended Hückel calculations are insensitive to some important contributions to electron energy which include electron correlation, relativistic and relaxation effects. Because of its success in predicting relative B.E.s in organic complexes (15), the extended Hückel formalism offers the best method available to calculate charge and binding energy for such large molecular systems as we deal with here, despite its limitations mentioned above.

Using these correlations and the XPS data from a number of inorganic iron-sulfur complexes we have interpreted the XPS spectra from the non-heme iron proteins. Where applicable, we also compare the results of other spectroscopic techniques with those of XPS.

The sulfur data are especially interesting. Rubredoxin, with no labile sulfur atoms and 4 cysteine sulfurs, shows one S2P photoelectron peak at 162.7 eV, which is relatively close to the value for S2P photoelectrons from clostridial apoferredoxin. Correlations between B.E. and calculated charge (as shown in Figure 5) indicate that a B.E. of 163 eV corresponds

to a sulfur charge of about zero. This is consistent with the apoferredoxin, which contains cysteine sulfurs. However, X-ray diffraction results (19) indicate the four sulfurs of oxidized rubredoxin are bound to iron in a tetrahedral arrangement, and the XPS of inorganic complexes show such sulfurs to exhibit typically an S2P photoelectron peak at about 161.5 eV (see Table III and Figure 4). Consequently, the rubredoxin S2P B.E. of 162.7 eV must be interpreted as an unusual bonding situation where the cysteine sulfur is weakly bonded to neutral iron such that little or no charge is effectively transferred between the two atoms, or, considering item 1c of Table IV, as cysteine sulfur bonded to iron in a positively charged complex wherein any negative charge on the sulfur would be neutralized. The peak at about 168 eV in the rubredoxin spectrum corresponds to the S2P electrons from the $SO_4^=$ ion, which is apparently present with this protein.

HIPIP, with four labile sulfur atoms and four cysteine sulfurs, yields two sulfur photoelectron peaks of approximately equal intensity at B.E.s of 162.9 eV and 161.5 eV. The value at 162.9 eV corresponds closely to that of the S2P photoelectrons from rubredoxin and is given a similar interpretation. As illustrated in Figure 4, the value of 161.5 eV corresponds more nearly to the typical value of an iron-bonded sulfur found in the iron-sulfur complexes of Table III. The sulfur associated with this B.E. is assumed to be the "labile" sulfur and to be bonded only to the iron and not to the protein. The third S2P peak at highest B.E. is assumed to originate from an oxidized sulfur species not associated with the active site.

Spinach ferredoxin, with two labile sulfur atoms and five cysteine sulfurs, exhibits a spectrum which can be decomposed into at least two

S2P photoelectron peaks in the approximate ratio of 5 to 2 (as determined by a computer analysis). Through a lorentzian curve fit, these peaks are determined to occur at 163.1 eV and 161.1 eV, respectively. The value at 163.1 eV is taken to correspond to that of rubredoxin and is interpreted similarly, while the value at 161.1 eV again corresponds more nearly to the sulfur of inorganic iron-sulfur complexes and is assigned to the "labile" sulfur.

Clostridial ferredoxin, with six to eight labile sulfurs and six to eight cysteine sulfurs, also can be decomposed into at least two photoelectron peaks in the approximate ratio of 4 to 3. It should be noted, however, that in at least one experiment with this protein, an intensity ratio of 1 to 1 was found. It is not certain which ratio is the more accurate. The B.E. value of 163.2 eV is interpreted in a manner similar to that of rubredoxin, while the value at 161.5 eV corresponds again to an iron-bonded sulfur found in the iron-sulfur complexes.

Curiously, the XPS spectrum of ammonium sulfate precipitated clostridial ferredoxin displayed only one S2P peak at 161.3 eV aside from a sulfate S2P peak at 168 eV. This could possibly be due to a difference in bonding between solution and crystallized ferredoxin. There is also the possibility that the spectral intensity at approximately 163 eV is due at least in part to cysteine groups in denatured protein since no samples attained 100% purity and surface decomposition would not be detected directly. Finally, it should again be noted that the intensity ratios given for the above protein spectra are only rough estimates based on the assumption that only two peaks are present; thus quantitative interpretation of sulfur content cannot be made with certainty.

Due to the ambiguities of peak position and the unspecified origin of spectral broadening, interpretation of the iron data is somewhat less certain than is the sulfur data. Rubredoxin, containing only one iron atom, yields a single Fe3P peak of normal half-width. The Fe3P B.E. of 54.6 eV is unusually high compared to those of the iron-sulfur complexes listed in Table III and Figure 4. EPR investigations of oxidized rubredoxin indicate that the iron is in the ferric state, and since X-ray diffraction data give a structure which would not be expected to delocalize charge to a great degree, the high Fe3P B.E. is compatible with the EPR interpretation. A complex such as shown in 1c of Table IV could give an XPS spectrum corresponding to that of rubredoxin, since the high positive charge on the iron should result in a relatively high Fe3P B.E., while the zero charge on the sulfur would correspond to an S2P B.E. of approximately 163 eV. HIPIP, clostridial ferredoxin and spinach ferredoxin have somewhat similar Fe3P B.E.s ranging from 53.0 to 53.6 eV. As seen in Figure 4, these values are much more consistent with those of the iron-sulfur complexes presented in Tables III and IV. X-ray diffraction data (21,22) indicate that these latter three proteins contain iron associated with S in Fe-S clusters. This type of chemical environment would most likely result in electron delocalization, and consequently it would be difficult to assign a specific oxidation state to the iron of these proteins. This electron delocalization would be consistent with the low Fe3P B.E.s exhibited by the proteins. Such close association of irons is also suggested by EPR and magnetic susceptibility studies (23-25). Interpreting EPR data from spinach ferredoxin (clostridial ferredoxin has a similar EPR spectrum), Brintzinger et al. (26) devised a model of an

iron-sulfur center as two iron-centered tetrahedra joined at an edge. Gibsen et al. (27), interpreting the same data, assumed that the active moiety contains, in the oxidized form, two high-spin Fe^{3+} irons which are anti-ferromagnetically coupled to form a singlet state. It has also been reported that oxidized clostridial ferredoxin gives a magnetic susceptibility per iron which shows a linear increase with temperature over the range 6 to 65°C, indicating strong anti-ferromagnetic coupling between irons (24). If the S" charge on model complex #2 from Table IV were more positive (and thus have a higher S2P B.E.) through perhaps a charged complex, then this type of model would be compatible with the XPS spectra of spinach and clostridial ferredoxin and HIPIP. The Fe3P photoelectron peak broadening can possibly be due to slightly different chemical environments of the iron atoms or to core polarization effects (12). Core polarization phenomena are due to electron exchange interactions between unpaired valence electrons and the electrons of the inner atomic shells. The net result is a splitting of core electron binding energies of several electron volts. Information concerning spin state and ligand arrangement is derived from the intensities and separation of the split photoelectron lines. However, the Fe3P peak broadening may simply result from the poor statistical resolution; thus, no definite interpretation can presently be attributed to this broadening.

The observation that both the iron and "inorganic" sulfur peaks are absent in the XPS spectra of apoferredoxin is consistent with the optical data, i.e., these constituents are associated with the chromophoric group in the native protein. Unlike optical spectroscopy, experimental difficulties mentioned above have thus far precluded assessment of the effects of reducing agents on the XPS spectra of the non-heme iron proteins.

CONCLUSION

The XPS data of the non-heme iron proteins have been interpreted with respect to hypothetical and synthesized iron-sulfur complexes. Where applicable these interpretations have been shown to be compatible with results from other spectroscopic techniques. Essentially we have found that the XPS data from rubredoxin, exhibiting relatively high B.E.s for the iron and sulfur atoms and only one sulfur peak, are compatible with a structure similar to item 1c of Table IV. On the other hand, the XPS data from the other three proteins investigated, exhibiting relatively low B.E.s for the iron atoms and two sulfur peaks, are more compatible with a structure similar to item 2 of Table IV. These interpretations are admittedly somewhat generalized, but can be used as a foundation for more conclusive work in the future.

This report has demonstrated the feasibility of using XPS for studying biological systems. Experimental limitations of spectral resolution and intensity should be overcome in order to yield much more information than presently is possible. For example, valuable information concerning ligand arrangements about an atom, electron distribution and spin state can be obtained by studying core polarization phenomenon of suitable complexes (12). One must always be concerned about the detrimental effects of radiation upon biological systems, and better methods should be developed to monitor the purity of a sample's uppermost layers. With improvements in equipment and technique, this spectral method should prove a valuable tool in probing biological systems.

REFERENCES

1. MALKIN, R., AND RABINOWITZ, J. C., Ann. Rev. Biochem., 36, 113 (1967).

2. KIMARA, T., Struct. Bonding (Berlin), 5 1 (1968).

3. TSIBRIS, J.C.M., AND WOODY, R. W., Coordination Chemistry Reviews, Elsevier Publishing Co., Amsterdam, 1970.

4. DER VARTANIAN, D. V., ORME-JOHNSON, W. H., HANSEN, R. E., AND BEINERT, H., Biochem. Biophys. Res. Commun., 26, 569 (1967).

5. SHETHNA, Y. I., WILSON, P. W., HANSEN, R., AND BEINERT, H., Proc. Nat. Acad. Sci. U.S.A., 52, 1263 (1964).

6. HAGSTROM, et al., in K. SIEGBAHN (Editor), Alpha- Beta- and Gamma-Ray Spectroscopy, Vol. 1, North-Holland, Amsterdam, 1968, p. 845.

7. SIEGBAHN, K., et al., ESCA--atomic, molecular, and solid state structure studied by means of electron spectroscopy, Almquist and Wiksella, Uppsala, 1967.

8. FADLEY, C. S., HAGSTROM, S.B.M., KLEIN, M. P., AND SHIRLEY, D. A., J. Chem. Phys., 48, 3779 (1968).

9. TAGAWA, K., AND ARNON, D., Nature, 195, 537 (1962). We are indebted to Mr. Alexander Sun for his patient instruction and aid in preparing spinach ferredoxin.

10. SIEGBAHN, K., NORDLING, C., AND HOLLANDER, J. M., Lawrence Radiation Laboratory Report, UCRL-10023.

11. KRAMER, L. N., AND KELIN, M. P., J. Chem. Phys., 51 #8, 3618 (1969).

12. FADLEY, C. S., Ph.D. dissertation, University of California, Berkeley, 1970, Lawrence Radiation Laboratory Report, UCRL-19535. (This program was developed by Claudette Rugge of the Lawrence Radiation Laboratory.)

13. GREENSTEIN, J. P., AND WINITZ, M., Chemistry of the Amino Acids, Vol. 1, John Wiley and Sons, Inc., New York, 1961, p. 683.

14. MALKIN, R., AND RABINOWITZ, J. C., Biochem. Biophys. Res. Commun., 23, 822 (1966).

15. KRAMER, L. N., AND KLEIN, M. P., Chem. Phys. Letters, 8 #2, 183 (1971).

16. HOFFMANN, R., AND LIPSCOMB, W. N., J. Chem. Phys., 36, 2179, 3489 (1962).

17. HOFFMANN, R., J. Chem. Phys., 39, 1397 (1963).

18. VAN DER VOORN, P. C., AND DRAGO, R. S., J. Amer. Chem. Soc., 88, 3255 (1966).

19. HERRIOTT, J. R., SIEKER, L. C., JENSEN, L. H., AND LOVENBERG, W., J. Mol. Biol., 50, 391 (1970).

20. CASTNER, T., et al., J. Chem. Phys., 32, 668 (1960).

21. STRAHS, G., AND KRAUT, J., J. Mol. Biol., 35, 503 (1968).

22. SIEKER, L. C., AND JENSEN, L. H., Biochem. Biophys. Res. Commun., 20, 33 (1965).

23. BEINERT, H., AND SANDS, R. H., Biochem. Biophys. Res. Commun., 3, 41 (1960).

24. ORME-JOHNSON, W. H., AND BEINERT, H., Biochem. Biophys. Res. Commun., 36, 337 (1969).

25. POE, M., PHILLIPS, W. D., McDONALD, C. C., AND LOVENBERG, W., Proc. Nat. Acad. Sci. U.S.A., 65, 797 (1970).

26. BRINTZINGER, H., PALMER, G., AND SANDS, R. H., Proc. Nat. Acad. Sci. U.S.A., 55, 397 (1966).

27. GIBSON, J. F., et al., Proc. Nat. Acad. Sci. U.S.A., 56, 987 (1966).

TABLE I

PROTEIN	M.W.	(1) No. of Fe (2) No. of S_i (inorg.) (3) No. of S_o (cysteine)	REDOX POTENTIAL	EPR	X-RAY DIFFRACTION (Fe-S moiety)
RUBREDOXIN	6,000	(1) 1 Fe (2) 0 S_i (3) 4 S_o	−57 mV	Oxidized: 4.3,9 Reduced: (none)	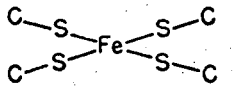
SPINACH FERREDOXIN	12,000	(1) 2 Fe (2) 2 S_i (3) 5 S_o	−430 mV	Oxidized: (none) Reduced: 1.89, 1.94, 2.01	Postulated 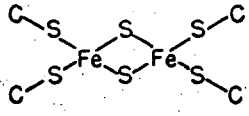
HIPIP	10,000	(1) 4 Fe (2) 4 S_i (3) 4 S_o	+330 mV	Oxidized: $g_{\parallel}$=2.12, $g_{\perp}$=2.04 Reduced: (none)	Unknown
CLOSTRIDIAL FERREDOXIN	6,000	(1) 6-8 Fe (2) 6-8 S_i (3) 8 S_o	−410 mV	Oxidized: (none) Reduced: 1.89, 1.96, 2.00	Unknown

XBL714-5123

Summary of important physical characteristics of the four non-heme iron proteins under investigation.

TABLE II

PROTEIN	STOICHIOMETRY OF Fe-S_i MOIETY	Fe3P B.E.	AREA RATIO	S2P B.E.	AREA RATIO
OXIDIZED RUBREDOXIN	1 Fe-O S_i 4 Cysteines	54.6 ± .4 eV	1	162.7 ± .3 eV	1
REDUCED HIPIP	4 Fe-4 S_i 4 Cysteines	53.0 ± .4 eV	1	162.9 ± .3 eV 161.5 ± .3 eV	1 1
OXIDIZED CLOSTRIDIAL FERREDOXIN	X Fe-X S_i 8 Cysteines (x = 6 to 8 atoms)	53.4 ± .4 eV	1	163.2 ± .3 eV 161.5 ± .4 eV	(approx) 4 3
OXIDIZED SPINACH FERREDOXIN	2 Fe-2 S_i 5 Cysteines	53.6 ± .5 eV	1	163.1 ± .4 eV 161.1 ± .4 eV	(approx) 5 2
APO CLOSTRIDIAL FERREDOXIN	0 Fe-0 S_i 4 Cystines	— — — —	—	163.2 ± .2 eV	1

XBL714-5124

Summary of the quantitative results from the XPS spectra of the non-heme iron proteins. The area ratios are only approx. values derived from lorentzian functions fitted to the XPS data.

TABLE III

MODEL COMPOUNDS	Fe3P B.E.(eV)	CALC. CHARGE	S2P B.E.(eV)	CALC. CHARGE
FeS_2	53.0	0.45	161.5	-0.22
FeS	—	0.43	160.7	-0.43
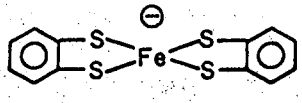	53.2	0.29	161.4	-0.43
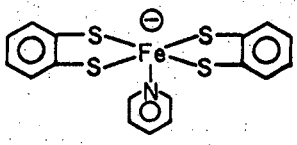	52.9	—	161.4	—
$KFeS_2$	—	0.35	161.1	-0.46
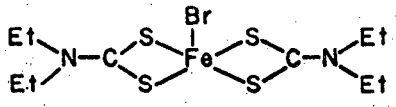	54.0	0.82	161.4	-0.3
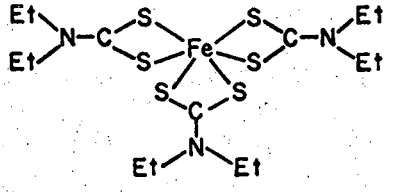	53.5	0.95	161.5	-0.3
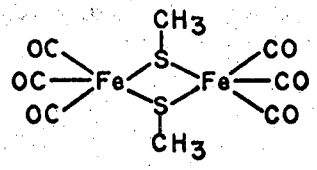	54.9	—	162.3	—
$(C_5H_5FeS)_4$	54.0	—	162.1	—

XBL714-5125

Measured Fe3P and S2P B.E.s and calculated charges of synthesized model iron-sulfur complexes. The B.E.s are reproducible to within .3 eV and the charges are self-consistent to within .05 charge units.

TABLE IV

MODEL COMPLEX	CALC. Fe CHARGE	CALC. S' CHARGE	CALC. S" CHARGE	BOND DIST. #1 (Å)	BOND DIST. #2 (Å)
(1) 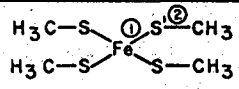					
(a) Tetrahedral, neutral	0.37	−0.22	—	2.3	1.82
(b) Tetrahedral, +2 complex	0.63	−0.06	—	2.3	1.82
(c) Tetrahedral, +3 complex	0.71	0	—	2.3	1.82
(2) 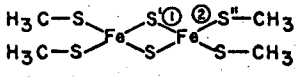					
Tetrahedral, neutral	0.66	−0.31	-0.32	2.24	2.44
(3) 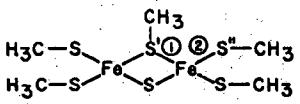					
Tetrahedral, neutral	0.64	+0.15	−0.23	2.24	2.44
(4) 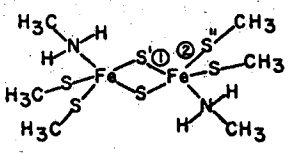					
Pseudotetrahedral, neutral	0.3	−0.6	+0.1	2.3	2.48

XBL714-5126

Calculated iron and sulfur charges of hypothetical model iron-sulfur complexes. The charges are self-consistent to within .05 charge units.

TABLE V

Measured and calculated electron binding energies and calculated charges for a diverse series of iron and sulfur compounds. The B.E.s are reproducible to within .3 eV and the charges are self-consistent to within .05 charge units.

No.	Molecule	Measured Fe3P B.E. (eV)	Calc. Fe3P B.E. (eV)	Calc. iron charge	Measured S2P B.E. (eV)	Calc. sulfur charge
1	FeF_6 (K_3FeF_6)	57.7	56.0	+1.81		
2	$FeO_4^{=}$ (K_2FeO_4)	57.7	56.1	+1.79		
3	$Fe(H_2O)_6^{+3}$ ($Fe_2(SO_4)_3 \cdot (NH_4)_2SO_4 \cdot 24H_2O$)	56.6		+1.51		
4	$Fe(H_2O)_6^{+2}$ ($FeSO_4(NH_4)_2SO_4 \cdot 6H_2O$)	54.2		+0.86		
5	$Fe(CN)_6^{-3}$ ($K_3Fe(CN)_6$)	55.0		+1.24		
6	$Fe(CN)_6^{-4}$ ($K_4Fe(CN)_6$)	54.0		+1.03		
7	Fe(metal)	52.4	52.0(def.)	0(def.)		
8	$Fe(C_5H_5)_2$	53.7	54.5	+1.00		
9	$Fe(C_5H_5)_2^{+} \cdot (NO_2)_3C_6H_2O^{-}$	54.9		+1.36		
10	$Fe(CO)_5$	54.0	54.7	+1.02		
11	$Fe_2(CO)_9$	54.6		+1.30		
12	FeS_2	53.0	53.3	+0.45	161.5	-0.22
13	$Fe(S_2CNEtEt)_3$	53.5		+0.95	161.5	-0.3
14	$FeBr(S_2CNEtEt)_2$	54.0	54.1	+0.82	161.4	-0.3
15	$Fe(S_2C_6H_3CH_3)_2^{-} \cdot N(n\text{-}C_4H_9)_4^{+}$	53.2		+0.29	161.4	-0.43
16	Ferrichrome A	54.9	55.5	+1.53		
17	Hemin Cl	54.2		+1.04		
18	Fe^{+3}Cl Phthalocyanine	54.4		+1.46		
19	$SO_4^{=}$				167.8	+1.86
20	$SO_3^{=}$				166.4	+1.40
21	CH_3SOCH_3				165.5	+0.70
22	CH_3SSCH_3				162.7	-0.13
23	CH_3SH				162.7	+0.09
24	FeS			+0.43	160.7	-0.43
25	KFeS2			+0.35	161.1	-0.46

FIGURE CAPTIONS

Fig. 1. Schematic outline of X-ray photoelectron method. A 2S electron is shown being ejected into the energy continuum by an X-ray photon.

Fig. 2. S2P photoelectron spectra of the four non-heme iron proteins under investigation and also that of clostridial apoferredoxin. The spectra have been fitted with lorentzian curves by means of a least squares computer analysis.

Fig. 3. Fe3P photoelectron spectra of the four non-heme iron proteins under investigation. The spectra have been fitted with lorentzian curves by means of a least squares computer analysis.

Fig. 4. Summary of the XPS data from Tables II, III, and IV. The curved lines within the semi-circles represent the error range of the corresponding binding energies of the samples. The data labeled M.C. are the model complexes found in Table IV and the B.E.s corresponding to the charges from Fig. 5.

Fig. 5. Plot of measured Fe3P B.E. and S2P B.E. versus calculated charge in iron and sulfur compounds chosen to represent a diversity of electronic environments. The line drawn through the iron data points is a least squares fit to the data from neutral molecules. The numbers associated with the data points correspond to the compounds listed in Table V.

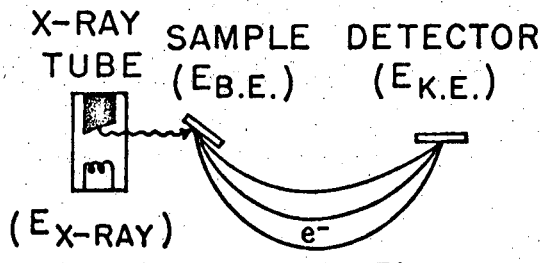

$$E_{B.E.} = E_{X\text{-}RAY} - E_{K.E.}$$
(Known) (Measured)

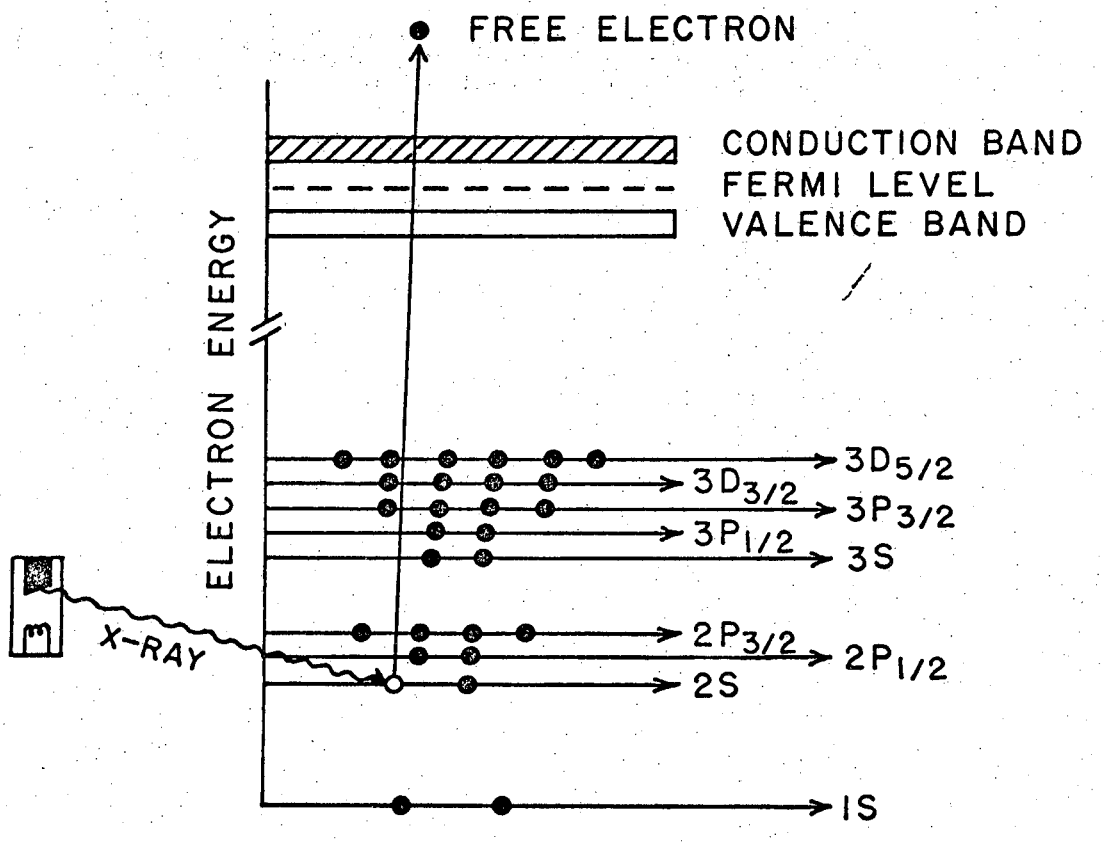

XBL 705-5218

Fig. 1

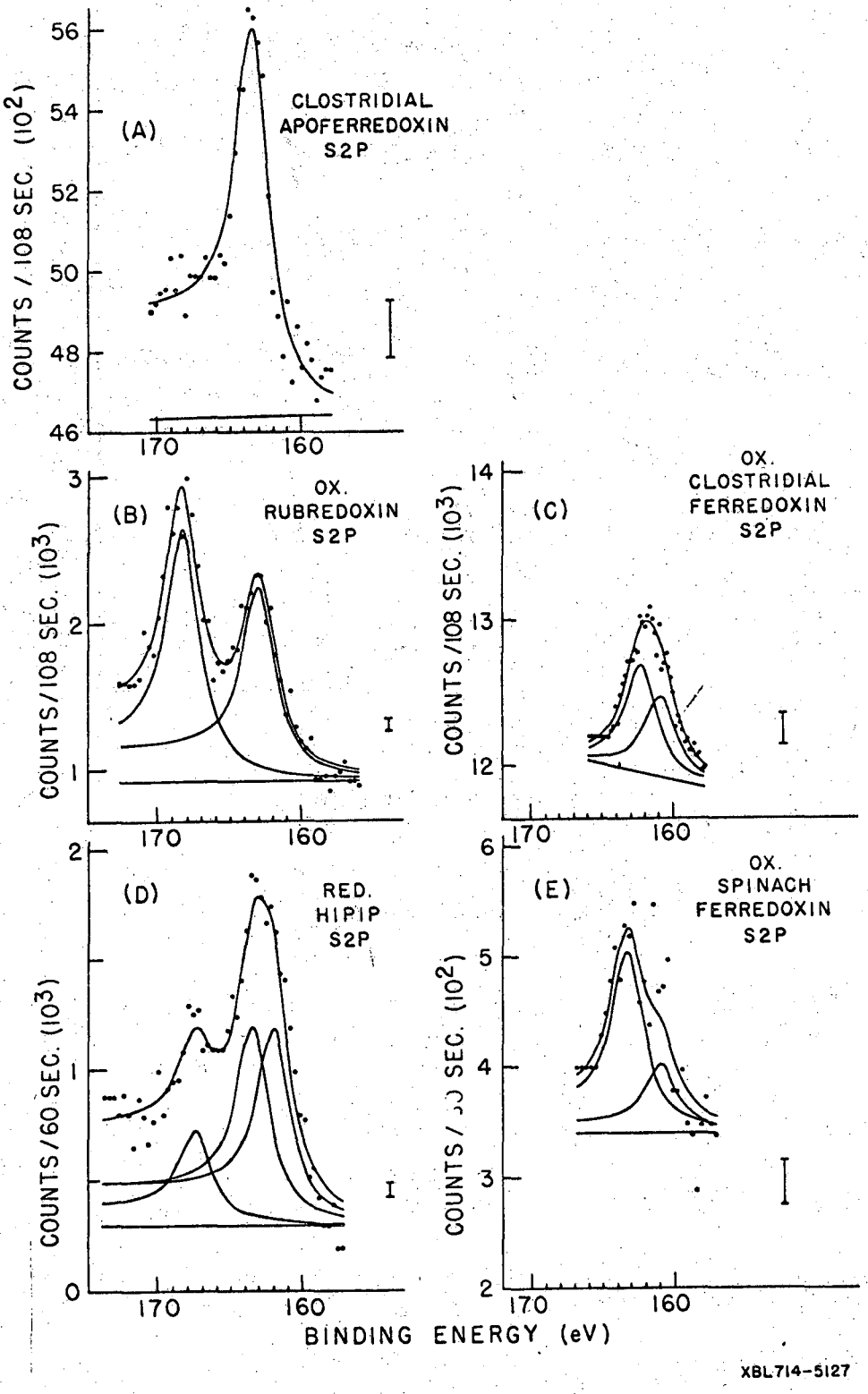
(A)
CLOSTRIDIAL APOFERREDOXIN S2P
COUNTS / 108 SEC. (10²)
(B)
OX. RUBREDOXIN S2P
COUNTS/108 SEC. (10³)
(C)
OX. CLOSTRIDIAL FERREDOXIN S2P
COUNTS/108 SEC. (10³)
(D)
RED. HIPIP S2P
COUNTS/60 SEC. (10³)
(E)
OX. SPINACH FERREDOXIN S2P
COUNTS / 60 SEC. (10²)
BINDING ENERGY (eV)
XBL714-5127

Fig. 2

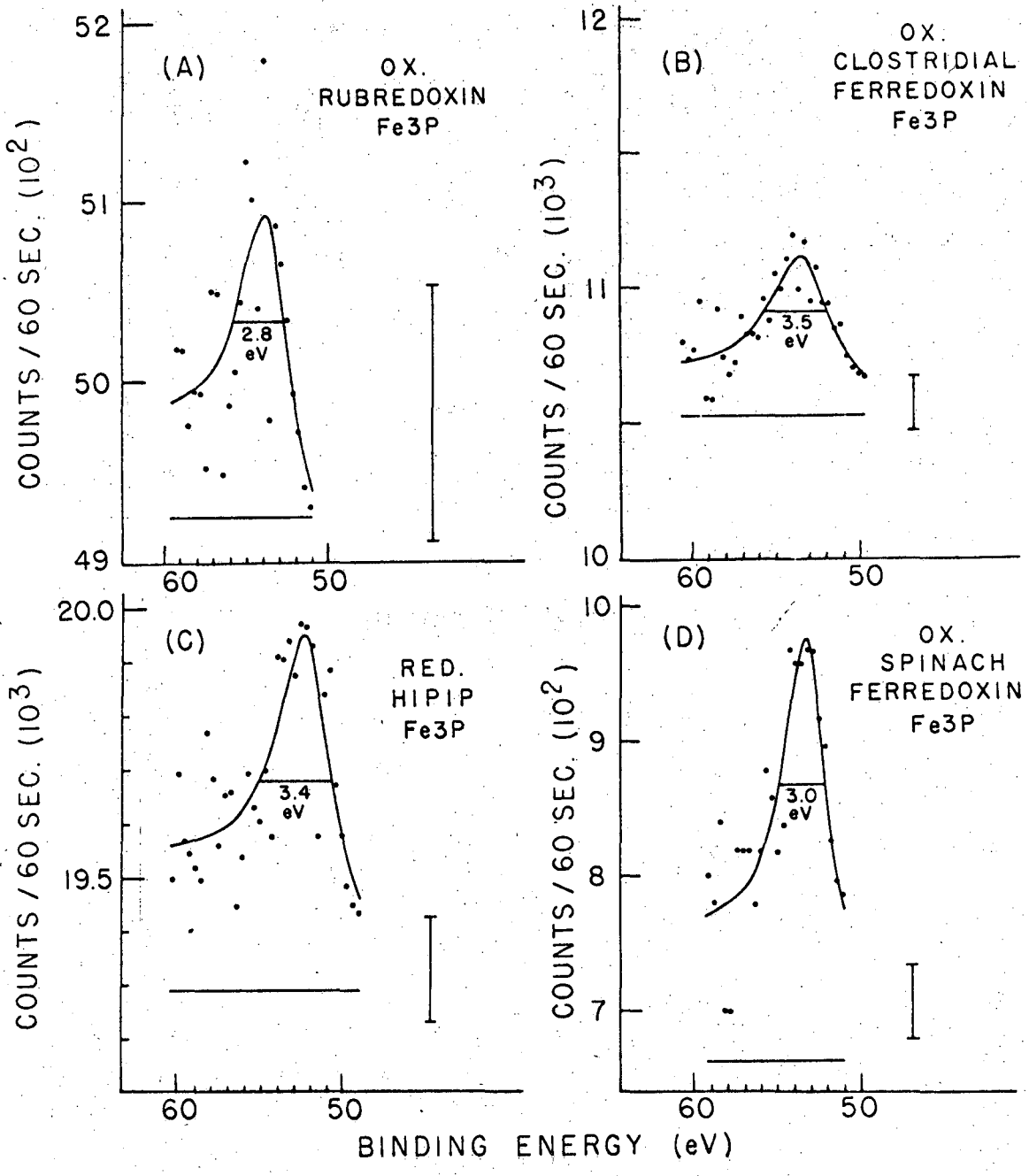

XBL714-5128

Fig. 3

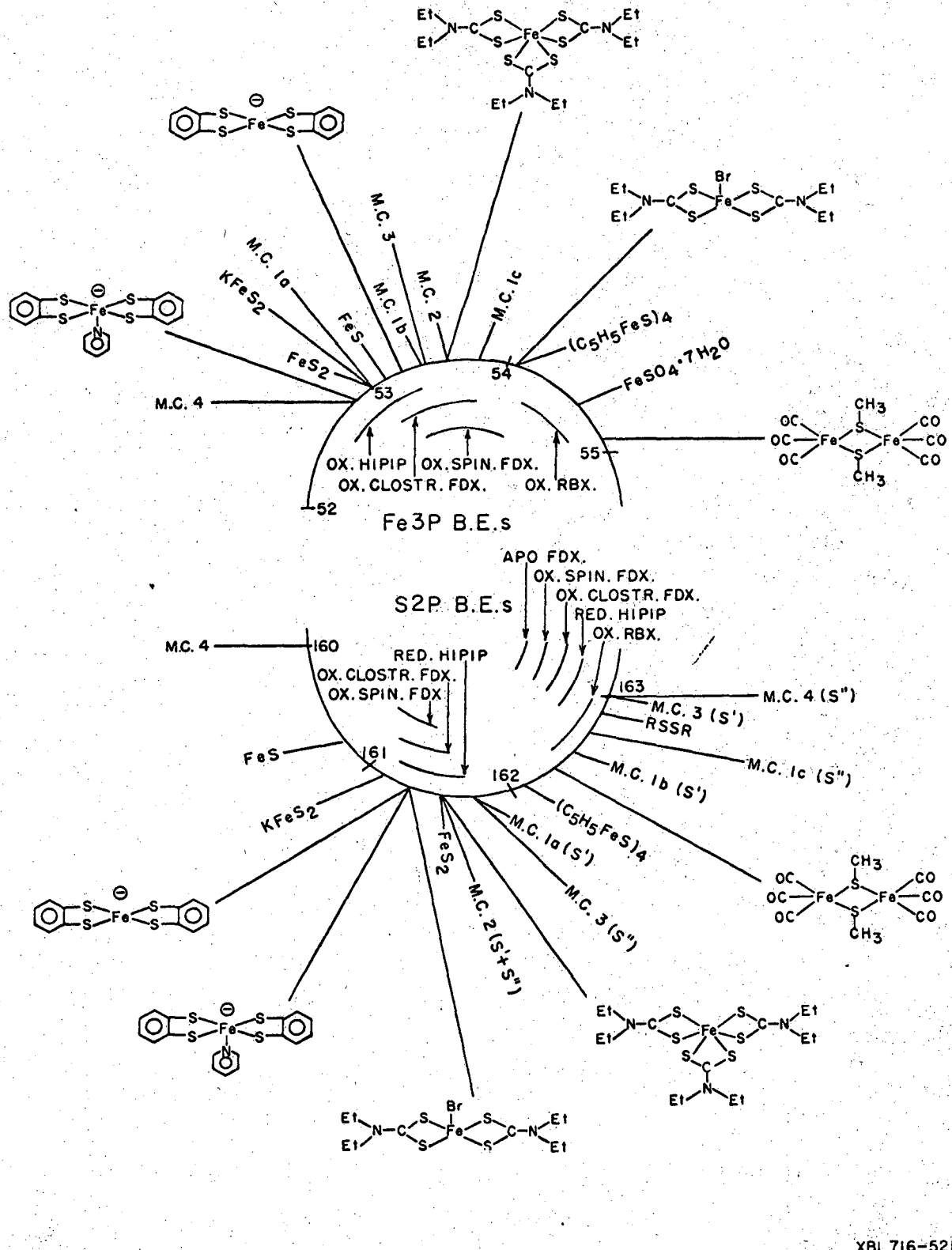

XBL716-5219

Fig. 4

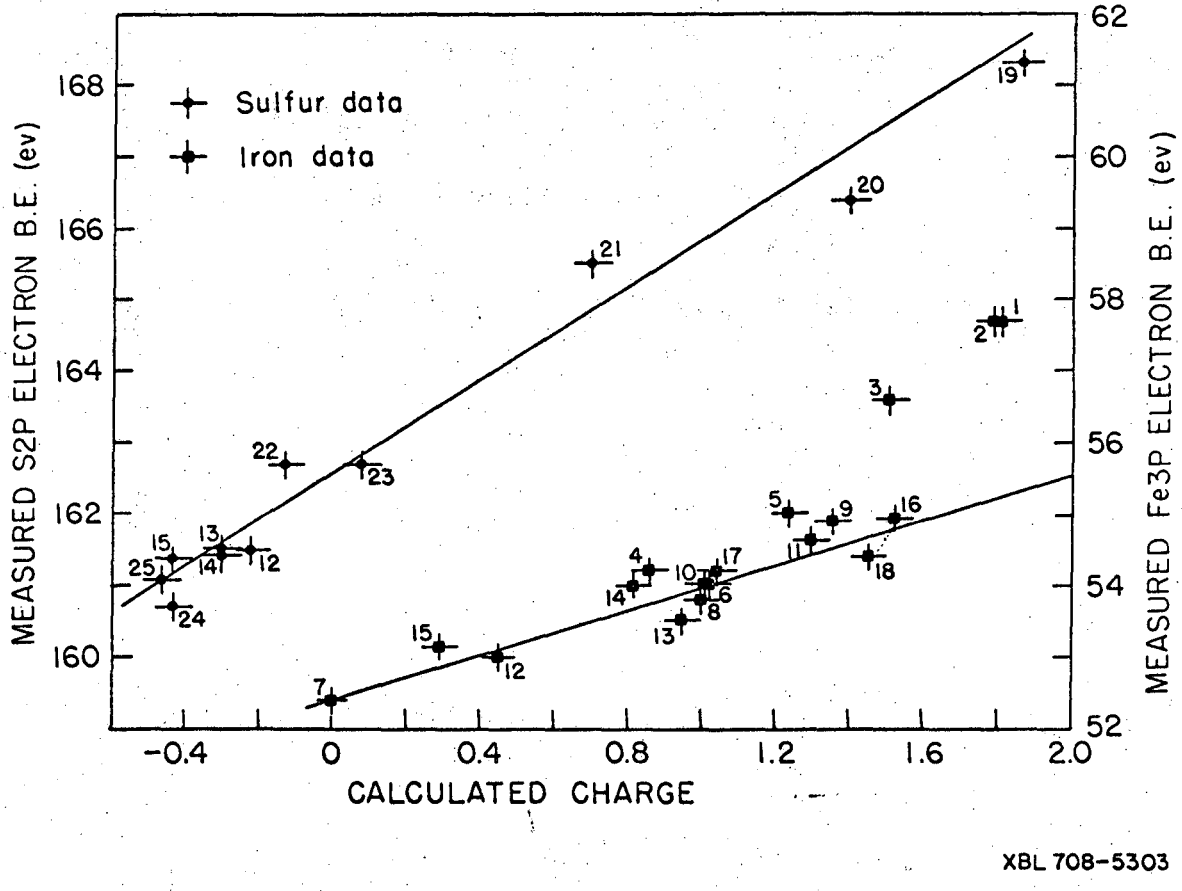
Sulfur data
Iron data
MEASURED S2P ELECTRON B.E. (ev)
MEASURED Fe3P ELECTRON B.E. (ev)
CALCULATED CHARGE
168
166
164
162
160
62
60
58
56
54
52
-0.4
0
0.4
0.8
1.2
1.6
2.0
XBL 708-5303

Fig. 5

TECHNICAL INFORMATION DIVISION
LAWRENCE RADIATION LABORATORY
UNIVERSITY OF CALIFORNIA
BERKELEY, CALIFORNIA 94720